

Subsolidus rubidium-dominant feldspar from the Morrua pegmatite, Mozambique: paragenesis and composition

D. K. TEERTSTRA, P. ČERNÝ AND F. C. HAWTHORNE

Department of Geological Sciences, University of Manitoba, Winnipeg, Manitoba, Canada R3T 2N2

ABSTRACT

At the Morrua pegmatite, Mozambique, alkali feldspar has replaced pollucite under low-temperature (250–150°C) hydrothermal conditions. Fluids invading a fracture system in pollucite formed round granular aggregates of (K-Rb)-feldspar in three stages: (1) a compositionally heterogeneous core of the feldspar cluster (+cookeite ± apatite) with 7–20 mol.% $\text{RbAlSi}_3\text{O}_8$, grading outward into a Rb-dominant feldspar with 66 mol.% $\text{RbAlSi}_3\text{O}_8$ (20 wt.% Rb_2O); (2) an intermediate layer of non-porous, inclusion-free, end-member K-feldspar; (3) an outer layer of porous end-member K-feldspar. Feldspars of all three stages seem to be monoclinic and disordered, with metastable sanidine structure. Zoning in K/Rb, preserved on a fine scale, was formed during growth at a temperature too low for subsequent alkali-cation diffusion or (Al,Si)-ordering.

KEYWORDS: K-feldspar, Rb-feldspar, rubidium, sanidine, granitic pegmatite.

Introduction

THE Morrua pegmatite, parental to the Rb-dominant feldspar described here, is a member of the Alto Ligonha pegmatite field in Mozambique (Correia Neves, 1981), related to late Pan-African granites dated at ~450 Ma (von Knorring and Condliffe, 1987). Morrua, hosted by medium-grade amphibolites, is a highly fractionated, zoned, spodumene-subtype pegmatite (Correia Neves, 1981), currently mined for tantalite.

Near-extreme fractionation of rare alkalis is documented in the Morrua pegmatite by the bulk composition of blocky microcline-perthite with 1.44 to 2.75 wt.% Rb and K/Rb variable from 7.4 to 3.8 (Correia Neves, 1981), and by the occurrence of associated pollucite (Khalili and von Knorring, 1976; Teertstra and Černý, 1997). This aluminosilicate of cesium marks the ultimate alkali fractionation, attained in only ~80 pegmatites worldwide (Teertstra, 1991). Such concentrations of Rb and Cs are also typical of other economically important pegmatites (Smeds and Černý, 1989): accumulation of pollucite may amount to 350,000 tons at 23.3 wt.% Cs_2O (Tanco in Manitoba; Černý *et al.*, 1996), and

Rb_2O may come close to 6 wt.% in bulk compositions of K-feldspar from near the core zones of these pegmatites (Red Cross Lake in Manitoba; Černý *et al.*, 1985; Černý, 1994).

A Rb-dominant feldspar of unknown structural state was recently found dispersed throughout pollucite in an unspecified pegmatite in the Kola Peninsula, Russia (Teertstra *et al.*, 1997), and a triclinic Rb-dominant feldspar, rubicline $(\text{Rb},\text{K})\text{AlSi}_3\text{O}_8$, was recently discovered in a pegmatite sample from Elba, Italy, as an exsolution product dispersed on a microscopic scale in Rb-bearing microcline (Teertstra *et al.*, 1998a). Here, we give the first description of a feldspar zoned in K/Rb which can be shown to have a low-temperature subsolidus hydrothermal origin, and which is probably highly disordered.

Experimental

Mineral compositions were measured using wavelength-dispersion (WDS) analysis on a CAMECA SX-50 electron microprobe (EMP) operating at 15 kV and 20 nA with a beam diameter of 5 μm . Using these conditions, gain or loss of alkali elements from the EMP-analysed volume is negligible. Data were reduced using the

PAP procedure of Pouchou and Pichoir (1985). Back-scattered electron (BSE) imaging, a technique sensitive to variation in mean atomic number, was used to examine compositional heterogeneity. Major elements were analysed using a glass of $\text{Rb}_2\text{ZnSi}_5\text{O}_{12}$ stoichiometry (Rb- $L\alpha$) and gem sanidine from Volkesfeld, Eifel, Germany (K- $K\alpha$, Al- $K\alpha$, Si- $K\alpha$) as standards. The procedure of Teertstra *et al.* (1998b) was used to measure accurately the composition of the sanidine and to provide conformity with ideal feldspar stoichiometry. Minor elements were measured using albite (Na- $K\alpha$), pollucite (Cs- $L\alpha$), fayalite (Fe- $K\alpha$), baryte (Ba- $L\beta$), SrTiO_3 (Sr- $L\alpha$) and VP_2O_5 (P- $K\alpha$) as standards. The elements Mg, Fe, Ti, F, P, Mn, Ga, Ca and Pb were sought but not detected in any generation of feldspar; limits of detection and additional experimental details are provided in Teertstra *et al.* (1998b).

Feldspar formulae were calculated on the basis of eight atoms of oxygen per formula unit (*apfu*). Monovalent and divalent cations were assigned to the *M*-site and higher-valency cations to the *T*-site of the general formula MT_4O_8 . Compositional vectors thereby directly correspond to the plagioclase-like substitution $(M^{2+}\text{Al})(M^{1+}\text{Si})_{-1}$, and to the 'excess'-silicon substitution $\square\text{Si}_4\text{O}_8$ (i.e. $\square\text{Si}(\text{KAl})_{-1}$). Comparison of the charge of the framework with the *M*-cation charge (M^+ =monovalent + $2 \times$ divalent cations) gives a trend for the incorporation of light-element *M*-cations, a compositional feature which cannot be

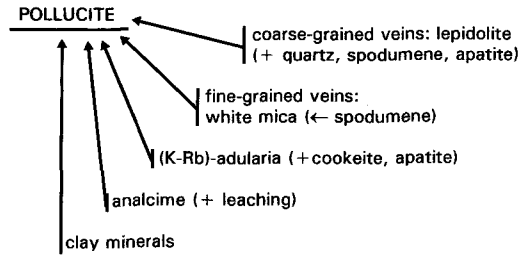


FIG. 1. Schematic sequence of alteration products of primary pollucite, arranged by paragenetic sequence and decreasing temperature of crystallization downwards.

measured directly by electron-microprobe analysis.

Below, the term (K,Rb)-feldspar is used for K-dominant compositions, and (Rb,K)-feldspar for Rb-dominant compositions; the term (K-Rb)-feldspar designates members of the solid-solution series. The terms Rbf and Csf signify the end-member components of ideal rubidium feldspar and cesium feldspar, respectively.

The (K-Rb)-feldspars and associated minerals

The genetically late, low-temperature feldspars examined here occur as part of a sequence of minerals formed by alteration of the Morrua pollucite (Fig. 1). In hand specimen, pollucite is white to colourless, and is penetrated by 2–3 mm-

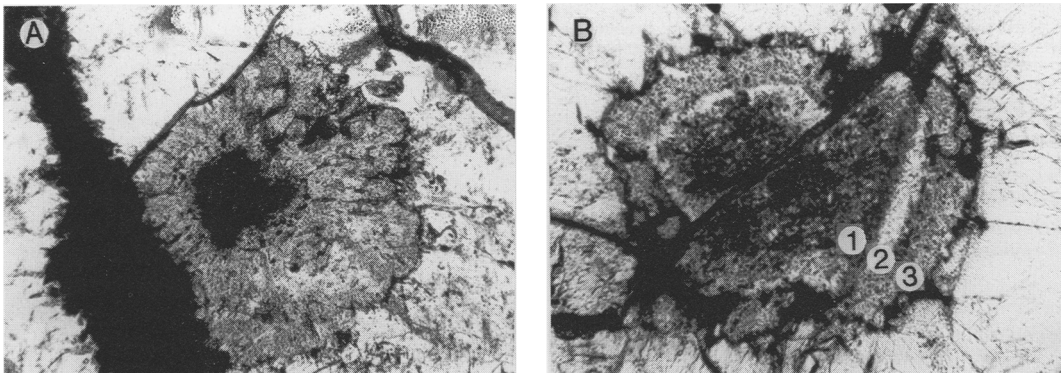


FIG. 2. (A) Round granular aggregate of (K-Rb)-feldspar (mottled grey) with a cookeite-rich core (black). The feldspar occurs between wide veins of lepidolite and thin veins of muscovite (black), and replaces pollucite (dirty white). The vertical edge of the photomicrograph (in plane-polarized light) is 0.5 mm. (B) Granular aggregate of (K-Rb)-feldspar on either side of a thin vein of fine-grained muscovite (vertical photo edge 0.5 mm, plane-polarized light). Three stages of growth are observed: (1) a black core with abundant cookeite \pm apatite; (2) an overgrowth of inclusion-free K-feldspar (white), and (3) an outer layer of porous K-feldspar.

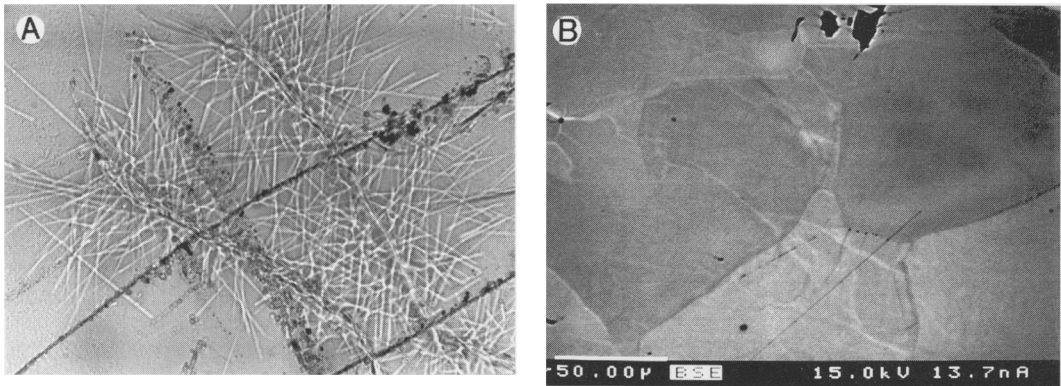


FIG. 3. (A) Leaching channels along fractures in pollucite (vertical photo edge 0.5 mm, plane-polarized light). (B) Back-scattered electron image (SX 50) of pollucite, with varying grey levels indicating minor variations in Na/Cs ratio among adjacent grains. The scale bar is 50 μm long.

wide veins of coarse-grained mauve lepidolite (\pm quartz, apatite and spodumene). Later veins of fine-grained white mica are partly replaced by fine-grained spodumene. Granular aggregates of feldspar, <1 mm in size, replace pollucite at its contact with the mica veins and also form spherical aggregates along fractures within the pollucite (Figs 2A,B). Microscopic leaching channels (<10 μm wide) extend into the pollucite from the surfaces of the feldspar and also from fractures

(Fig. 3A). Late analcimization of pollucite seems to be associated with the formation of these channels. Fractures in pollucite are filled locally with a buff-to-white clay mineral, and surfaces are stained with black and red Mn- and Fe-bearing oxides. The primary pollucite shows only slight compositional heterogeneity (Fig. 3B). The mean Si/Al ratio is 2.47, the CRK index ($=100(\text{Cs}+\text{Rb}+\text{K})/(\text{Cs}+\text{Rb}+\text{K}+\text{Na}+\text{Ca})$ at.) is 87.7, and the Rb_2O content is 0.32 wt.% (cf. Teertstra

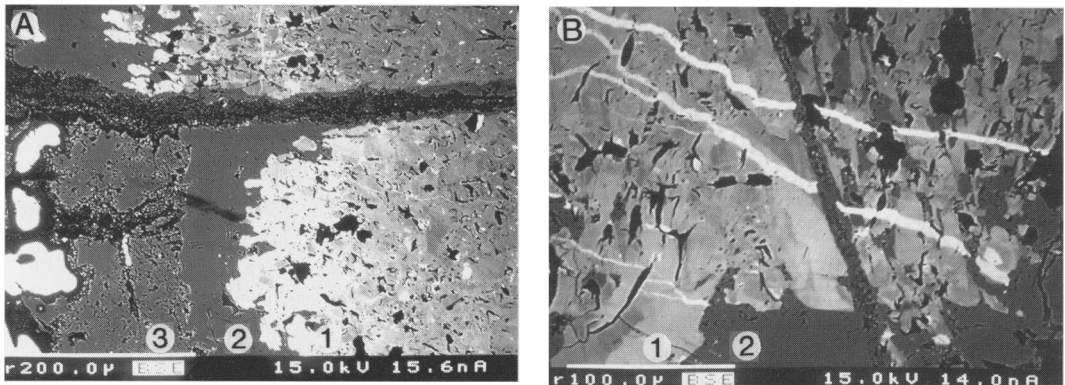


FIG. 4. (A) Back-scattered electron image (SX 50) of a part of the area shown in Fig. 2B with (K-Rb)-feldspar overgrowing a thin vein of fine-grained muscovite (black, horizontal). The core of the feldspar aggregate is to the right, growth progressed toward the left. The core contains cookeite (black flakes) and is progressively enriched in Rb (bright area near centre, 1). The Rb-dominant margin of the core is overgrown by layers of clear and micropore-rich Or_{100} feldspar (black, 2 and dark grey, 3, respectively). The micropore-rich K-feldspar is associated with analcimization (black) of pollucite (white round grains along left edge of the image). The scale bar is 200 μm long. (B) Back-scattered electron image (SX 50) of veinlets of (Rb,K)-feldspar (white), cross-cutting Rb-variable adularia (mottled dark to light grey, 1) with inclusions of cookeite (black flakes); the aggregate is rimmed and cut by late Or_{100} adularia (black, 2). The scale bar is 100 μm long.

TABLE 1. Representative compositions of (K-Rb)-feldspar from Morrua, Mozambique

Oxide	Stage-1						Stage 2	Stage 3
	1	2	3	4	5	6	7	8
SiO ₂	63.12	63.26	61.18	59.69	57.20	59.77	65.06	65.57
Al ₂ O ₃	17.73	17.34	17.09	16.99	16.69	16.32	18.24	17.56
Na ₂ O	0.02	0.01	0.02	0.01	0.00	0.00	0.02	0.00
K ₂ O	14.62	12.71	9.22	8.30	5.07	6.45	16.89	16.31
Rb ₂ O	3.09	6.22	12.37	14.37	19.81	16.62	0.00	0.00
Cs ₂ O	0.00	0.29	0.29	0.38	0.59	0.39	0.00	0.00
SrO	0.06	0.01	0.08	0.03	0.08	0.19	0.04	0.01
BaO	0.17	0.07	0.03	0.04	0.12	0.00	0.00	0.03
Sum	99.28	100.03	100.32	99.90	99.65	99.84	100.40	99.68
Cation contents based on 8 atoms of oxygen								
Si	3.005	3.023	3.010	2.993	2.976	3.024	3.006	3.039
Al	0.995	0.977	0.991	1.004	1.024	0.973	0.993	0.959
Na	0.002	0.001	0.002	0.001	0.000	0.000	0.002	0.000
K	0.888	0.775	0.579	0.531	0.337	0.416	0.995	0.964
Rb	0.095	0.191	0.391	0.463	0.663	0.540	0.000	0.000
Cs	0.000	0.006	0.006	0.008	0.013	0.005	0.000	0.000
Sr	0.002	0.000	0.002	0.001	0.003	0.005	0.001	0.000
Ba	0.003	0.001	0.001	0.001	0.002	0.000	0.000	0.001
ΣM	0.989	0.975	0.981	1.005	1.018	0.970	0.998	0.965
M^+	0.994	0.977	0.984	1.007	1.024	0.970	0.999	0.966
TO_2^-	0.995	0.977	0.991	1.006	1.024	0.973	0.993	0.960
ΣT	4.000	4.000	4.002	4.000	4.000	3.999	3.999	3.999

- 1–2. Main area of stage-1 (K-Rb)-feldspar
 3–5. Outer Rb-rich margins of stage-1 feldspar
 6. (Rb,K)-feldspar vein cutting stage-1 feldspar
 7. Stage-2 non-porous K-feldspar
 8. Stage-3 microporous K-feldspar

and Černý, 1997, for additional details on pollucite constitution).

Three main stages can be observed in the formation of feldspar that replaces pollucite (Fig. 4A). Stage-(1) feldspar is heterogeneous with patchy and variable Rb content, and is associated with cookeite and apatite. From core to rim, K/Rb decreases, as does the abundance of cookeite inclusions. Rare 10 µm-wide veins of Rb-rich feldspar crosscut the early feldspar (Fig. 4B). Stage-(1) feldspar is locally veined, replaced but mainly overgrown by a 100 µm-thick layer of non-porous stage-(2) K-feldspar which corresponds to end-member Or₁₀₀. The final, stage-(3) layer is porous but also consists of end-member Or₁₀₀ K-feldspar. This latest stage of feldspar growth is closely associated with leached and cation-exchanged pollucite.

Optical data for the feldspars could not be readily determined because of their abundant inclusions and the very small grain size. The stage-(1) feldspar has sweeping extinction but appears untwinned. The stage-(2) and stage-(3) feldspar overgrowths appear twinned; however, the quasi-twin planes radiate from the core of the feldspar assemblage and indicate subparallel growth of untwinned individuals rather than twinning.

The stage-(1) feldspar that replaces pollucite is an almost pure member of the (K-Rb)AlSi₃O₈ series, with up to 66 mol.% Rbf. Compositions of the stage-(2) and stage-(3) feldspars correspond to the almost pure end-member K-feldspar. Representative compositions are given in Table 1. Within error, values of Al are equal to values of the *M*-cation charge (Fig. 5A). Silicon

Rb-DOMINANT FELDSPAR FROM MOZAMBIQUE

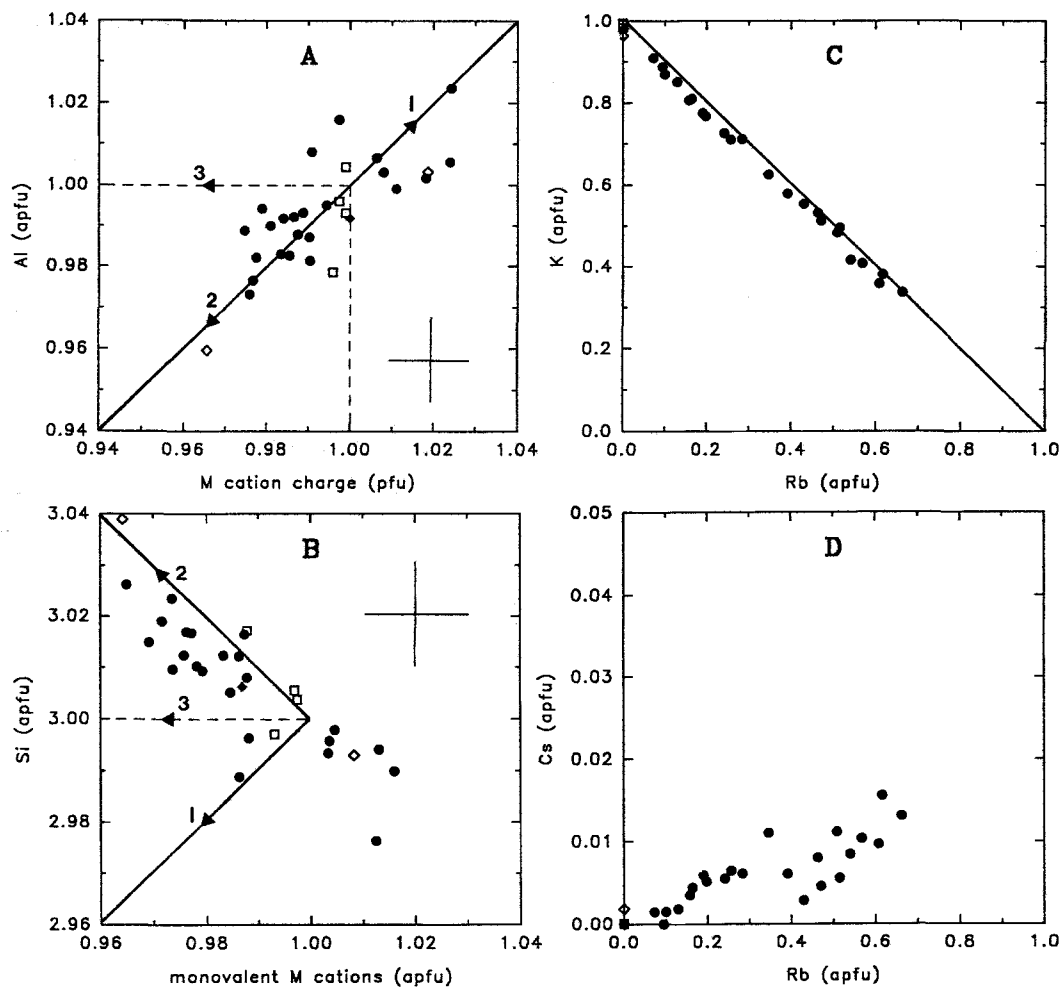


FIG. 5. Element variation in (K-Rb)-feldspars: (A) Al vs. M -cation charge with a 1:1 trend line; (B) Si vs. sum of monovalent M cations; (C) K vs. Rb, with a line indicating $\Sigma M = 1$; (D) Cs vs. Rb. Symbols: ● stage-1, □ stage-2, ◇ stage-3 feldspar. Crosses indicate the precision (4σ) of measurement for the sanidine standard. Vectors indicate (1) plagioclase-type substitution, (2) $\square\text{Si}_4\text{O}_8$ substitution and (3) apparent cation deficiency.

increases with decreasing sum of the monovalent M cations in stage-(1), -(2) and -(3) feldspars (Fig. 5B). As no divalent cations were detected in analysis, this trend probably represents substitution of up to 4 mol.% $\square\text{Si}_4\text{O}_8$. Mean values of $M' = 0.994(15)$, $7\text{O}_2 = 0.993(13)$, $\text{Si} = 3.007(13)$ and $\Sigma T = 4.000(2)$ a.p.f.u. indicate good agreement with this substitution. A plot of K vs. Rb shows substitution along a line from 1 K to 1 Rb a.p.f.u. (Fig. 5C). Substitution of Cs increases with Rb, but is less than 0.02 a.p.f.u. (Fig. 5D).

The substitution of $\square\text{Si}_4\text{O}_8$, confirmed recently in feldspars of pegmatitic origin (Teertstra *et al.*, 1998b), seems to be somewhat dispersed in Fig. 5B. However, the trend is clearly defined in Figs 6A,B. Values of $\text{Si} > 3$ and $\text{Al} < 1$ show a distinct correlation with sums of M -cations, extending as far as 0.96 a.p.f.u. The analytical precision (4σ) is 0.01 a.p.f.u. for Si, Al and ΣM , and the analytical results which deviate from integral stoichiometry by amounts greater than these are significant. Some of the data extend to

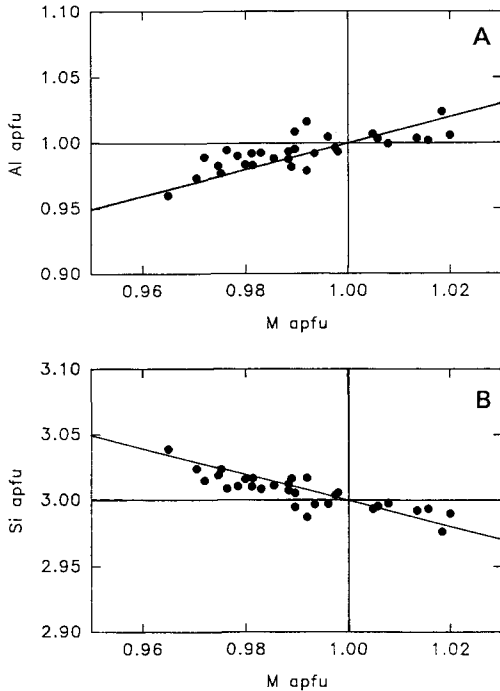


FIG. 6. Variation of Al (A) and Si (B) with the content of monovalent cations, supporting the $\square\text{Si}_4\text{O}_8$ substitution.

values of $\text{Si} < 3$ and $\text{Al} > 1$, with $\Sigma M > 1.01$ to 1.02 a.p.f.u., suggesting slight inaccuracy in this set of data. However, even if the data are accurate within only 2% (absolute), the trend of the data is well-defined within an analytical precision of 1% (4σ) (Teertstra *et al.*, 1998b).

Discussion

The Morrua pegmatite can be estimated to have crystallized between ~ 650 and $\sim 450^\circ\text{C}$ and 2–4 kbar, as established by detailed studies of similar bodies with high contents of Li, Rb, Cs, B and F (London, 1986; Chakoumakos and Lumpkin, 1990). The presence of primary spodumene limits the pressure of consolidation to ≥ 2.6 kbar (London, 1984). Blocky (K,Na,Rb)-feldspar and associated primary pollucite probably crystallized near the lower end of the above temperature range; pollucite is a near-solidus phase, as documented by its paragenetic relationships (Černý, 1982) and by experimental work (Henderson and Manning, 1984). Crystallization of these minerals generated the matrix for the observed subsolidus processes.

The close association of hydrothermal K-feldspar with end-member pollucite at other localities, such as Greenwood (Maine) and Ambatonfinondrahana (Madagascar) suggests an approximate temperature of co-precipitation of $300\text{--}200^\circ\text{C}$, with subsequent analcimization at $200\text{--}100^\circ\text{C}$ (Teertstra and Černý, 1995). Because the Morrua feldspar is associated with analcime (formed by cation exchange of pollucite) rather than with reprecipitated end-member pollucite, the temperature of precipitation may be in the intermediate range of $250\text{--}150^\circ\text{C}$ (cf. Teertstra *et al.*, 1993; Teertstra and Černý, 1997). This estimate is supported by the association of the feldspar with cookeite (Vidal and Goffé, 1991), by the lack of Rb or K diffusion (which is restricted at low temperature; Gilletti, 1994), and by the end-member compositions of stage-(2) and stage-(3) K-feldspar, which are to be expected at low-temperature extrapolation of the Or-Ab solvus. The equilibrium Rb/K distribution coefficient between K-feldspar and aqueous fluid at 180°C is 0.28 (Pauwels *et al.*, 1989). This indicates that the parent fluids for the Morrua feldspars were considerably enriched in Rb. The sequence of alteration of pollucite and the progressive stages of (K-Rb)-feldspar crystallization indicate that the late-stage pegmatite fluids at this locality had the following sequence of activities: $\text{Rb} < \text{Li} < \text{K} < \text{Na}$.

The preservation of fine-scale growth zoning and layering in K/Rb indicates that the feldspar formed at a temperature too low for subsequent solid-state diffusion, or fluid-promoted cation exchange. Such a low temperature of crystallization is characteristic of the morphologically distinct variety of K-feldspar, adularia. The Morrua feldspars examined here are anhedral, but, like most samples of adularia, are virtually Na-free and non-perthitic (Worden and Rushton, 1992; Dong and Morrison, 1995; Teertstra *et al.*, 1998b); paragenetically, they are also entirely analogous to euhedral adularia replacing pollucite at other localities (e.g. Luolamäki in Finland; Teertstra, 1997).

Low temperature of crystallization favours monoclinic symmetry and (Al,Si)-disorder which, in most cases, is preserved even in the presence of abundant fluid (Černý and Chapman, 1984, 1986; Černý, 1994). In particular, high-sanidine structure was documented for K-dominant adularia replacing pollucite at other localities (Černý and Chapman, 1984; Teertstra *et al.*, 1998b). Attempts at separation of the Morrua

adularia for X-ray powder diffraction were not successful. However, optical behaviour of the Morrua feldspars corresponds to that of monoclinic phases; consequently, a disordered sanidine-type structure can be expected for both K-dominant and Rb-dominant feldspars.

Acknowledgements

This work was supported by the Natural Sciences and Engineering Research Council of Canada Research and Major Installation Grants to P.Č., by NSERC Research, Equipment and Infrastructure Grants to F.C.H., and by a University of Manitoba Duff Roblin Fellowship to D.K.T. Thanks go to the late O. von Knorring for the samples examined, to C.M.B. Henderson for the Rb standard and to H. Wondratschek for the Eifel sanidine. Constructive reviews by Dr Martin Lee and the editors were much appreciated.

References

- Černý, P. (1982) Mineralogy of rubidium and cesium. In *Granitic Pegmatites in Science and Industry* (P. Černý, ed.), Mineral. Assoc. Canada Short-Course Handbook, **8**, 149–61.
- Černý, P. (1994) Evolution of feldspars in granitic pegmatites. In *Feldspars and Their Reactions* (I. Parsons, ed.), NATO ASI Series C, **421**, 501–40.
- Černý, P. and Chapman, R. (1984) Paragenesis, chemistry and structural state of adularia from granitic pegmatites. *Bull. Minéral.*, **107**, 369–84.
- Černý, P. and Chapman, R. (1986) Adularia from hydrothermal vein deposits: extremes in structural state. *Canad. Mineral.*, **24**, 717–28.
- Černý, P., Penttinghaus, H. and Macek, J.J. (1985) Rubidian microcline from Red Cross Lake, north-eastern Manitoba. *Bull. Geol. Soc. Finland*, **57**, 217–30.
- Černý, P., Ercit, T.S. and Vanstone, P.J. (1996) Petrology and mineralization of the Tanco rare-element pegmatite, southeastern Manitoba. *Field Trip Guidebook A4*, Geol. Assoc. Canada — Mineral. Assoc. Canada Annual Meeting Winnipeg, Manitoba, 63 pp.
- Chakoumakos, B.C. and Lumpkin, G.R. (1990) Pressure-temperature constraints on the crystallization of the Harding pegmatite, Taos County, New Mexico. *Canad. Mineral.*, **28**, 287–97.
- Correia Neves, J.M. (1981) *Pegmatitos Graníticos. Morfologia, Mineralogia, Geoquímica, Gênese, Metalogênese*. Habil. thesis, Universidade Federal de Minas Gerais, A1–R23.
- Dong, G. and Morrison, G.W. (1995) Adularia in epithermal veins, Queensland: morphology, structural state and origin. *Mineral. Deposita*, **30**, 11–9.
- Giletti, B.J. (1994) Isotopic equilibrium/disequilibrium and diffusion kinetics in feldspars. In *Feldspars and Their Reactions* (I. Parsons, ed.), NATO ASI Series C, **421**, 351–82.
- Henderson, C.M.B. and Manning, D.A.C. (1984) The effect of Cs on phase relations in the granite system: stability of pollucite. *Nat. Env. Res. Council, Progr. Exper. Petrol.*, **25**, 41–2.
- Khalili, H. and von Knorring, O. (1976) Pollucite from some African and Scandinavian pegmatites. *Inst. African Geol. Leeds Univ., Ann. Rept.*, 1976, 59–60.
- London, D. (1984) Experimental phase equilibria in the system $\text{LiAlSiO}_4\text{-SiO}_2\text{-H}_2\text{O}$: a petrogenetic grid for lithium-rich pegmatites. *Amer. Mineral.*, **69**, 995–1004.
- London, D. (1986) Magmatic-hydrothermal transition in the Tanco rare-element pegmatite: evidence from fluid inclusions and phase-equilibria experiments. *Amer. Mineral.*, **71**, 376–95.
- Pauwels, H., Zuddas, P. and Michard, G. (1989) Behaviour of trace elements during feldspar dissolution in near-equilibrium conditions: Preliminary investigation. *Chem. Geol.*, **78**, 255–67.
- Pouchou, J.L. and Pichoir, F. (1985) 'PAP' (phi-rho-Z) procedure for improved quantitative microanalysis. In *Microbeam Analysis* (J.T. Armstrong, ed.) San Francisco Press, 104–6.
- Smeds, S.-A. and Černý, P. (1989) Pollucite from the Proterozoic petalite-bearing pegmatites of Utö, Stockholm archipelago, Sweden. *Geol. Foren. Forh.*, **111**, 361–71.
- Teertstra, D.K. (1991) *Compositional heterogeneity and alteration of pollucite*. Unpubl. M.Sc. thesis, Univ. Manitoba, Winnipeg.
- Teertstra, D.K. (1997) *Reactions of (K-Rb)-feldspars from rare-element granitic pegmatites*. Unpubl. Ph.D. thesis, Univ. Manitoba, Winnipeg.
- Teertstra, D.K. and Černý, P. (1995) First natural occurrences of end-member pollucite: A product of low-temperature reequilibration. *Eur. J. Mineral.*, **7**, 1137–48.
- Teertstra, D.K. and Černý, P. (1997) The compositional evolution of pollucite from African granitic pegmatites. *J. Afr. Earth Sci.*, **25**, 317–31.
- Teertstra, D.K., Černý, P. and Hawthorne, F.C. (1997) Rubidium-rich feldspars in a granitic pegmatite from the Kola Peninsula, Russia. *Canad. Mineral.*, **35**, 1277–81.
- Teertstra, D.K., Černý, P., Hawthorne, F.C., Wang, Lu-Min, Pier, J. and Ewing, R.C. (1998a) Rubicline, a new feldspar from San Piero in Campo, Elba, Italy. *Amer. Mineral.*, **83**, 335–9.
- Teertstra, D.K., Hawthorne, F.C. and Černý, P. (1998b)

- Identification of normal and anomalous compositions of minerals by electron-microprobe analysis: K-rich feldspar as a case study. *Canad. Mineral.*, **36**, 87–95.
- Teertstra, D.K., Lahti, S.I., Alviola, R. and Černý, P. (1993) Pollucite and its alteration in Finnish pegmatites. *Bull. Geol. Surv. Finland*, **368**, 39 pp.
- Vidal, O. and Goffé, B. (1991) Cookeite $\text{LiAl}_4(\text{Si}_3\text{Al})\text{O}_{10}(\text{OH})_8$: Experimental study and thermodynamic analysis of its compatibility relations in the $\text{Li}_2\text{O}-\text{Al}_2\text{O}_3-\text{SiO}_2-\text{H}_2\text{O}$ system. *Contrib. Mineral. Petrol.*, **108**, 72–81.
- von Knorring, O. and Condliffe, E. (1987) Mineralized pegmatites in Africa. *Geol. J.*, **22**, 253–70.
- Worden, R.H. and Rushton, J.C. (1992) Diagenetic K-feldspar textures: a TEM study and model for diagenetic feldspar growth. *J. Sed. Petrol.*, **62**, 779–89.
- [Manuscript received 18 June 1998;
revised 3 August 1998]